International Journal of Control, Automation and Systems 15(1) (2016) 73-84
http://dx.doi.org/10.1007/s12555-016-0487-7
ISSN:1598-6446 eISSN:2005-4092
http://www.springer.com/12555

Auxilio: A Portable Cable-driven Exosuit for Upper Extremity Assistance

Igor Gaponov, Dmitry Popov, Seung Jun Lee, and Jee-Hwan Ryu*

Abstract: This paper introduces a fully portable, lightweight exosuit-type device for shoulder and elbow assistance. The main motivation of this research was to design a portable upper limb exosuit capable to assist dynamic rehabilitation tasks where patient can involve trunk motions and overground movements (e.g., during pick-and-place tasks). The proposed system provides assistance for shoulder flexion and abduction, as well as for elbow flexion. The mechanism is driven by DC motors which are worn on the wearer's back, and the power is transferred from the actuators to the arm by means of cable-driven transmission. The unique features of the proposed exosuit are the absence of rigid links or joints around the arm, high compliance and portability. This paper describes operating principle and kinematic model of the proposed exosuit and provides force analysis and experimental evaluation of the manufactured device. As the result of this work, we performed a simulation of rehabilitation scenario with the developed wearable prototype.

Keywords: Assistive device, cable-driven actuation, exosuit, upper extremity rehabilitation.

1. INTRODUCTION

Movement disorders of the upper extremities severely impede the independence of affected subjects and decrease their quality of life. Such disorders may occur as a result of traumas, degenerative deceases, stroke, aging, and other reasons. One of the most common procedures to restore the functionality of upper extremities is physical therapy, and there have been an increased amount of research efforts directed into development of assistive robotic systems for upper limb rehabilitation in the recent decades.

Kiguchi *et al*. [1] developed an assisting system for shoulder movements with 2 degree of freedom (DOF). Sulzer *et al*. [2] designed an end-effector-based elbow assisting system providing one degree of freedom for physical therapy. Rosati *et al*. [3] developed a 5 DOF assisting system for both elbow and shoulder movements. Carignan *et al*. [4] developed a 5 DOF prototype for assisting shoulder, elbow and forearm movements. There are also several commercially available products, for instance, a 3 DOF device for shoulder and elbow movements assistance [5] and the Myomo e100 elbow assistant system [6].

However, most of those systems do not provide enough mobility and work space to perform such tasks as pick and place object over the distance as well as they restrict banding, seating and other trunk involving motions. Overcoming such limitations would enable a new specter of work for therapists. At the same, intense repetitions of rehabilitation activities are burdensome for the therapists, and because of the economic factors, the duration of primary rehabilitation is decreasing [7]. It can also be inconvenient or not feasible at all and time-consuming for the patients to commute to hospitals or therapy centers in order to undergo the required daily exercise routine. Therefore, there is currently a need in highly portable, inexpensive, and easily adjustable devices for upper extremity assistance which could enable new rehabilitation approaches and home-centered rehabilitation [8].

Several research groups attempted to design upper limb assistance devices with light wearable parts, which were driven by pneumatic actuators and McKibben muscles [9, 10]. Although these devices provide assistance for shoulder and elbow joints, the need in a heavy external power source impedes their portability severely. Existing portable devices are usually limited to elbow therapy and do not provide assistance for the shoulder joint [8, 11]. Two comprehensive overviews of state-of-the art devices for upper extremity assistance and rehabilitation are provided in [7] and [12].

In this paper, we propose a fully portable exosuit for shoulder and elbow movements' assistance. The proposed

Manuscript received August 2, 2016; revised October 28, 2016; accepted October 29, 2016. Recommended by Guest Editor Sungwan Kim. This work was partially supported by the project "Development of core teleoperation technologies for maintaining and repairing tasks in nuclear power plants" funded by the Ministry of Trade, Industry and Energy of S. Korea, the Industrial Strategic Technology Development Program (10052967) funded by the Ministry of Trade, Industry and Energy of S. Korea, and by National Research Foundation of Korea (NRF) grant funded by the Korea government (MSIP)(No. NRF-2013R1A2A1A03069658).

Igor Gaponov, Dmitry Popov, Seung Jun Lee, and Jee-Hwan Ryu are with the School of Mechanical Engineering, Korea University of Technology and Education, 1600 Chungjeolno, Cheonan, Chungnam, Korea (e-mails: {igor, dmitry, kor9431, jhryu}@koreatech.ac.kr).
* Corresponding author.

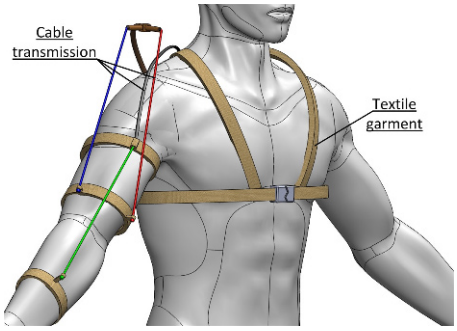

(a)

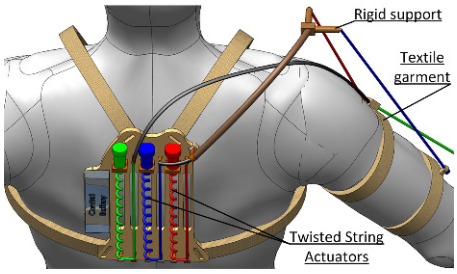

(b)

Fig. 1. Concept design of the proposed exosuit.

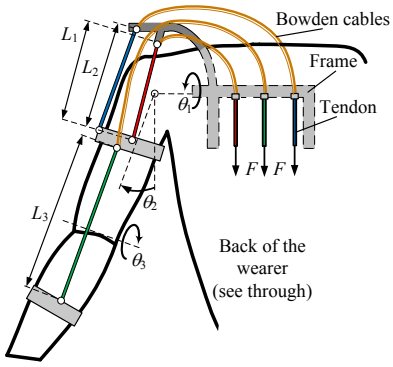

Fig. 2. A schematic representation of the proposed Auxilio upper-arm exosuit.

Fig. 3. Close-up view of the elbow harness.

novel exosuit is light, easily adjustable and not restricted by a bulky power source. The mechanism employs conventional DC motors and provides assistance in 3 degrees of freedom, namely, shoulder flexion and abduction and elbow flexion. In order to decrease the wearer's fatigue, we moved the actuators weight away from the arm and placed them remotely on the patient's back. To transfer the motion from motors to the arm we employ cable-driven transmission. The tendons (cables) are attached to the arm by means of a custom-designed textile garment with adjustable bands worn around the elbow joint. Substitution of conventional rigid links with textile components makes the overall system lighter. In addition, we employed twisted strings in the capacity of motor gears, which allowed us to introduce more compliance and further decrease the weight of the device.

The rest of the paper is organized as follows: Section 2 describes the proposed exosuit design in details. Section 3 is concerned with the kinematics and force analysis of the device, while Sections 4 and 5 are dedicated to experimental evaluation of the performance of the exosuit. Section 6 concludes the paper.

2. DESIGN CONCEPT

In this section, we discuss the design concept and provide a detailed description of the portable exosuit developed for shoulder and elbow assistance. The second part of this section presents the working principle of twisted string actuator and reason of its implementation.

2.1. Design concept of the exosuit

Light weight, adjustable structure, high degree of flexibility and portability of the power source were the crucial requirements in the design of the proposed device. In order to develop the device with desired properties, we selected DC motor-based actuators over pneumatic and hydraulic ones, moved all actuators, control hardware and batteries to the frame worn on the patient's back, and substituted all rigid joints and links by a soft harness system.

In such configuration, the arm is actuated by several tendons passing from the pulleys located above the shoulder (for shoulder joint actuation) and on the upper arm (for elbow flexion) to respective insertion points at the arm. The tendons (Dyneema strands with low friction coefficient and high stiffness) are guided through Bowden sheaths on their way from the actuators to the arm. Bowden cables help to remove any possible interference between the tendons and the human body during operation. The human skeleton itself provides rigid support. Although the developed tendon-driven system might appear less favorable in terms of accuracy and stiffness when compared to conventional rigid exosuits, it imposes less constraints on the arm movement and is lighter and more compact.

We decided to use a flexible harness with band adjustment to connect the tendons to the arm since it can be easily fitted to different arm girths (Fig. 3). The harness has a symmetrical design which allows wearing it on both

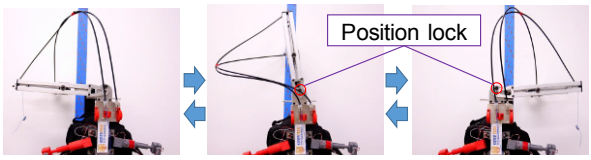

Fig. 4. Flipping of the shoulder support module.

arms. It also allows unconstrained elbow flexion and provides easy tension adjustment options. Design of efficient and comfortable harness for exosuit systems in general is a challenging task and requires a separate thorough investigation which we are planning to address in the future. However, having an offset between the shoulder and cable mounts drastically reduces shear forces applied to the garment while pulling and therefore does not require significant tightening of the harness for secure anchoring. Additionally, to reduce compression of the bands, we have anchored the upper arm band with a glove-like harness worn around the hand by means of adjustable cables. All these points simplify harness design and allow the hand to rest in the harness while being lifted upwards by two cables.

Being a cable-driven exosuit, the device is completely transparent when the motors are turned off in their initial position, and the wearer can move the arm freely without experiencing much fatigue added by the exosuit due to the low weight of the harness. On the other hand, this approach introduces such challenges as cable slack or over-tensioning. We have equipped the device with easily adjustable anchor-type cable locks so that the cable length can be varied from patient to patient without the need of any tools or changes in control strategy. Once the patient wears the system, an assistant can adjust cable length in order to remove slack or to prevent over-tensioning. We believe that minimal positioning errors originating due to the flexibility of the device are acceptable for such rehabilitation tasks as mirroring or moving the arm in a 3-dimensional space. If the slack causes visible positioning errors, the assistant should be able to adjust cable tension accordingly. Normally, the speeds of the arm positioning in the selected rehabilitation procedures are comparatively low and safe for the wearer, which gives the assistant enough time to address any cable issues. If the proposed device is adopted for tasks of home-based rehabilitation, slack mitigation control strategy will be developed.

Additionally, the proposed cable-driven design allows to use one set of pulleys and cables in order to assist either left or right arm of the patient (Fig. 4). The arm harness is also designed in such a way that it can be easily switched from left to right arm. The Bowden cables are mounted on the shoulder support unit via rotational joints which allows their free rotation without entangling or increase in bending angle. This overall concept reduces the cost and weight of the system as well as simplifies device workspace management for the therapists.

The present setup only provides pulling-up motion (extension and abduction), while it is assumed that the opposing arm motion is caused by gravity. In case when the arm is required to be actuated in a bidirectional way, additional tendons can be attached antagonistically to the same arm band on the opposite side of the arm. Both shoulder and elbow flexion actuators can be readily augmented to support the extension in that fashion, however, shoulder adduction might require a more complex mechanical design and cable routing technique.

With the proposed device, we targeted 3 of the 4 degrees of freedom of the elbow and shoulder, excluding elbow pronation-supination DOF. These degrees of freedom were selected for rehabilitation as they are responsible for covering most of the workspace of the healthy arm and are essential for hand positioning in space. As for the degrees of freedom of the wrist, in this work we were mainly concerned with gross arm rehabilitation as opposed to hand rehabilitation, and a separate wrist and hand rehabilitation device might be needed for this purpose.

2.2. Challenging issues

During the development of Auxilio, we have faced the following challenges:

- *Coupled tendons*: a change in length of a single tendon in the shoulder joint affected both joint coordinates.
- *Flexibility* of the device can negatively affect overall positioning accuracy.
- *Position of pulleys:* the placement of the pulleys that the tendons pass through should be optimized in order to increase the workspace and decrease required motor torques.

During this work, we solved the coupling issue of the shoulder joint tendons by constraining the tendons to operate in the mutually orthogonal planes by exosuit design and developing an accurate mathematical model of the device. Regarding the increased flexibility of the device, we attempted to mitigate its negative effect on accuracy by placing the actuators on a rigid frame located on the patient's back and developing a sling-like harness anchored around the elbow joint in order to avoid squishy soft areas and to prevent slipping of the bands during motion. Finally, we performed force analysis of the device in order to estimate which pulley positions would be optimal in terms of required motor torque for every point in the workspace of the exosuit.

2.3. Twisted string actuator

Twisted string actuator (TSA) is a powerful, compact, light, quiet, and compliant actuator, in which a string twisted by an electric motor contracts and acts as a gear. When having the string attached to an electrical motor at

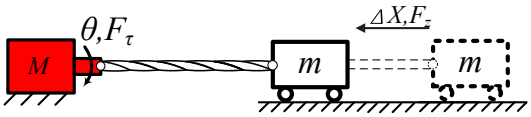

Fig. 5. Working principle of a twisted string actuator.

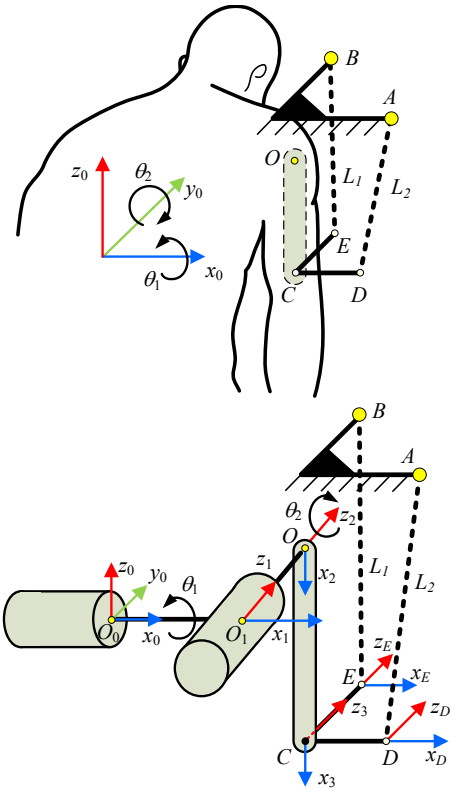

Fig. 6. Schematic placement of the cable support unit (top) and kinematic scheme of the shoulder joint. Angles θ_1 and θ_2 correspond to shoulder flexion and abduction, respectively.

one end and to a load on the other, the rotation imposed to the string by the motor will reduce the length of the string, resulting in the translational motion of the load (Fig. 2). Kinematics of such actuators are briefly described in the next section, and for more details the reader may refer to [13, 14].

In our approach, twisted string actuator was chosen for several reasons. First of all, it is a DC-motor based actuator that does not require a bulky external power source and therefore does not restrict system portability. At the same time, TSAs do not require the use of gears between the motors and the strings and therefore they are beneficial in terms of weight and cost. Secondly, twisted string actuators are inherently compliant, which makes a TSA-based system safer for human-robot interaction.

In total, there are 3 twisted string actuators implemented in the Auxilio device, which allows to position the arm in a 3-dimensional space. The following section presents kinematics of a twisted string actuator and of the proposed exosuit.

3. KINEMATICS OF THE EXOSUIT

The following subsection briefly describes the kinematics of TSA. Next, we provide the derivation of kinematic relations for the shoulder joint and its force analysis, and the section is concluded by elbow kinematics.

3.1. Twisted string kinematics

In a TSA, contraction of a string as the result of twisting can be calculated as follows [15]:

$$\Delta X = \sqrt{L^2 + \lambda^2 r^2} - L - \frac{F_z}{K}, \tag{1}$$

where L is the length of the string in the untwisted state, λ is the angle of twisting, r is the radius of a single string or bundle of strings, K is its tensile stiffness coefficient and F_z is the applied workload force, which in our case was generated by the human arm. However, the stiffness coefficient of the strings we used for our applications was typically of the order of 10^4-10^5 N/m, and therefore the last term F_z/K in model (1) can be neglected for simplicity.

3.2. Kinematics of the shoulder part

In order to derive the kinematics of the device, we represent human shoulder joint and upper-arm as a kinematic chain shown schematically in Fig. 6.

Working principle of the shoulder joint of Auxilio is as follows: Two TSAs located on the exosuit's frame change the length of the tendons between points $A-D$ and $B-E$, respectively. Therefore, contraction or extension of the tendons will result in the change of moduli of vectors $||BE||$ (for string 1) and $||AD||$ (for string 2). For the sake of brevity, these lengths are hereafter referred to as L_1 and L_2, respectively. The change of tendon lengths L_1 and L_2 will cause the 2-DOF shoulder joint to move, with the values of angles θ_1 and θ_2 uniquely determined by the lengths L_1 and L_2.

The inverse kinematics task of the designed shoulder joint can be formulated as follows : given the desired shoulder angles θ_1 and θ_2, determine the lengths of the strings L_1 and L_2 required to bring the arm to desired position.

In order to solve the inverse kinematics problem, we need to be able to calculate position of point C as a function of joint variables θ_1 and θ_2. The point C is assumed to be located at some point at center of the upper arm cross-section, while points D and E are situated on the arm's exterior. The coordinates of points D and E can be found consecutively through homogeneous transformations (e.g., using Denavit-Hartenberg convention), pro-

Table 1. Denavit-Hartenberg parameters of the shoulder joint.

Frames	θ	d	a	α
1 (O_1)	0	0	0	$-\pi/2+\theta_1$
2 (O_2)	$\pi/2+\theta_2$	0	0	0
3 (O)	0	0	l	0
C-D	$-\pi/2$	0	$\|\|CD\|\|$	0
C-E	$-\pi/2$	$\|\|CE\|\|$	0	0

Table 2. Mechanical parameters of the shoulder joint (values are in cm).

l	CD, CE	point A pos.	point B pos.
11	6	$[10.8, 0, 16.5]^T$	$[0, 19.2, 16.5]^T$

vided all lengths are known and remain constant. Once the global coordinates of points D and E are determined, one can find the lengths of tendons L_1 and L_2 by finding the vector norms $||EB||$ and $||DA||$, correspondingly.

In order to simplify solving the kinematics problem, we introduce coordinate frames in accordance with the Denavit-Hartenberg (DH) convention, as shown in Fig. 6. The obtained DH parameters of the coordinate frames are given in Table 1. Parameter l is the length of the upper arm link between points O and C, which is considered to be constant. It should be noted that the lengths $||O_0O_1||$ and $||O_1O||$ are considered to be zero. The values of actual mechanical parameters of the experimental setup are summarized in Table 2.

As a result, one can find the coordinates of all points using conventional DH transformation, which is omitted in this paper for the sake of brevity. Positions of points D and E can be both calculated then with respect to point C, e.g.

$$ {}^{O}\mathbf{H}_D = {}^{O}\mathbf{H}_C \cdot {}^{C}\mathbf{H}_D, \tag{2} $$

$$ {}^{O}\mathbf{H}_E = {}^{O}\mathbf{H}_C \cdot {}^{C}\mathbf{H}_E, \tag{3} $$

where ${}^{i}\mathbf{H}_j$ denotes homogeneous transformation matrix of coordinate frame j with respect to frame i.

After the coordinates of points D and E are calculated, with position of points A and B known, one can calculate the required lengths of tendons as $L_1 = ||BE||$ and $L_2 = ||AD||$, which concludes solving the kinematics of the developed shoulder joint.

3.3. Force analysis

A schematic force diagram used for the shoulder force analysis is presented in Fig. 7. After projecting the exosuit structure on plane y_0z_0 and solving kinematics for any given values of shoulder angles θ_1 and θ_2, one can obtain the coordinates of points C, D, E (tendon attachment points) and coordinate of the center of gravity G. Therefore, one can find the vectors along which tendon forces

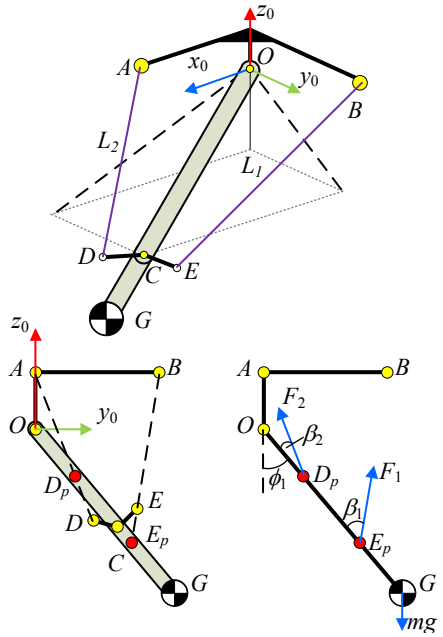

Fig. 7. Force analysis scheme: a general schematic representation of the arm structure (top) and a projected view on the y_0z_0 plane.

F_1 and F_2 act on the same plane y_0z_0. Translating these forces along their respective lines of action until the intersection with the upper arm OC, one obtains points D_p (for the force F_2) and E_p (for F_1). The coordinates of these points can be found as follows:

$$ Dp = \begin{bmatrix} y_c \\ z_c \end{bmatrix} \cdot k_d^{yz}, \tag{4} $$

$$ Ep = \begin{bmatrix} y_c \\ z_c \end{bmatrix} \cdot k_e^{yz}, \tag{5} $$

where

$$ k_d^{yz} = \frac{y_a \cdot z_d - z_a \cdot y_d}{-y_c \cdot (z_a - z_d) + z_c \cdot (y_a - y_d)}, \tag{6} $$

$$ k_e^{yz} = \frac{y_b \cdot z_e - z_b \cdot y_e}{-y_c \cdot (z_b - z_e) + z_c \cdot (y_b - y_e)}. \tag{7} $$

After the coordinates of points D_p and E_p in the XY-plane are calculated according to (4)-(5), one may find projections of the angles between the link and the respective tendons β_1 and β_2 applying the law of cosines to triangles OBE and ODA, correspondingly:

$$ \beta_1^{yz} = \arccos\left(\frac{||OE_p^{yz}||^2 + ||BE_p^{yz}||^2 - ||OB_p^{yz}||^2}{2 \cdot ||OE_p^{yz}|| \cdot ||BE_p^{yz}||} \right), \tag{8} $$

$$ \beta_2^{yz} = \arccos\left(\frac{||OD_p^{yz}||^2 + ||AD_p^{yz}||^2 - ||OA_p^{yz}||^2}{2 \cdot ||OD_p^{yz}|| \cdot ||AD_p^{yz}||} \right). \tag{9} $$

From now on, the force balance equation in the y_0z_0 plane can be written as follows:

$$F_1 \sin\beta_1^{yz}||OE_p^{yz}|| + F_2 \sin\beta_2^{yz}||OD_p^{yz}|| = mg||OG^{yz}|| \sin\phi_1, \quad (10)$$

where F_1 and F_2 are tendon forces required to hold the arm at the shoulder angle ϕ_1, m is the mass of the arm, and g is gravity constant. Terms with the superscript $|\cdot|^{yz}$ denote that these are projections onto the y_0z_0 plane.

Similarly, one can find the projections of the angles β_1 and β_2 onto the XZ-plane to derive the second equation for force analysis:

$$F_1 \sin\beta_1^{xz}||OE_p^{xz}|| + F_2 \sin\beta_2^{xz}||OD_p^{xz}|| = mg||OG^{xz}|| \sin\phi_2. \quad (11)$$

where ϕ_2 is the angle between the link OC and axis z_0 in the x_0z_0 plane. It should be noted that the absolute shoulder angles ϕ_1 and ϕ_2 should not be confused with the relative shoulder angles θ_1 and θ_2 described in the previous subsection: Although angles ϕ_1 and θ_1 coincide, the values of ϕ_2 and θ_2 can be different if $\theta_1 \neq 0$. The angles ϕ_1 and ϕ_2 can be calculated either from the orientation of point C found after solving shoulder kinematics or simply by $\phi_1 = \tan^{-1}(y_c/z_c), \phi_2 = \tan^{-1}(x_c/z_c)$, where x_c, y_c, z_c are the 3-dimensional coordinates of point C.

Equations (10) and (11) can be therefore written as follows:

$$[A] \cdot \{F\} = \{b\}, \quad (12)$$

with matrix $[A]$ and vectors $\{F\}$ and $\{b\}$ found as

$$[A] = \begin{bmatrix} \sin\beta_1^{yz} \cdot ||OE_p^{yz}||, & \sin\beta_2^{yz} \cdot ||OD_p^{yz}|| \\ \sin\beta_1^{xz} \cdot ||OE_p^{xz}||, & \sin\beta_2^{xz} \cdot ||OD_p^{xz}|| \end{bmatrix},$$

$$\{F\} = \begin{bmatrix} F_1 \\ F_2 \end{bmatrix},$$

$$\{b\} = \begin{bmatrix} mg \cdot ||OG^{yz}|| \cdot \sin\phi_1 \\ mg \cdot ||OG^{xz}|| \cdot \sin\phi_2 \end{bmatrix}.$$

From now on, equation (12) can be readily solved in order to obtain the values of tendon forces F_1 and F_1 required to hold the arm in position defined by the angles ϕ_1 and ϕ_2.

3.4. Experimental evaluation of force analysis

In this subsection, we present the results of force analysis for shoulder joint actuation performed on the mechanical dummy arm testbed. Results of the force analysis provide the insights which can be essential for design of the proposed exosuit. Firstly, by knowing tendon force required to hold the arm at a given point of workspace for a given device configuration, we can estimate the maximum required motor torques and thus select appropriate actuators. Secondly, efficiency of the implemented force transmission system can be estimated through the force analysis. Lastly, we can evaluate the relation between the required pulling force and positions of pulleys A and B. The latter analysis can help to minimize required motor torques and to extend operation time of the exosuit via optimal selection of the pulley positions.

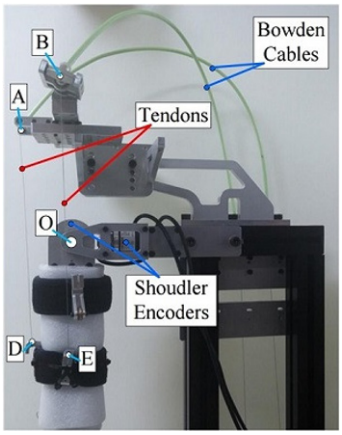

Fig. 8. General view of the dummy mechanical arm.

A custom dummy arm prototype shown in Fig. 8 was designed and manufactured for the force analysis. The mechanical shoulder joint incorporated two rotary encoders (Autonics E40H12-5000) which measured the shoulder angles θ_1 and θ_2, as shown in Fig. 8. Two Maxon RE30 motors equipped with 18-to-1 gear ratio reducers and encoders (L type, 1024 CPT) were installed on a rigid frame to actuate the tendons L_1 and L_2. Sava metal cables were traveling from the motors shaft to the arm band through the Bowden sheaths in order to minimize the friction along their path. The Bowden cables were attached to the frame at one end and to the points A and B at the shoulder side on the other end. Positions of points A and B were made mechanically adjustable in order to perform an experimental analysis of optimal pulley placement in terms of required motor torques.

In order to verify the analysis performed in Subsection 3.3, we installed load cells to each of the 2 tendons driving the shoulder and applied some pulling force while recording the position of the shoulder joint by encoders. Several combinations of the locations of pulleys A and B were tested, as the design of the dummy arm testbed enabled easy adjustment of pulleys' position.

Fig. 9 presents the comparison between theoretical and experimental values of tendon pulling forces and shoulder angles. The theoretical data were calculated using the force model (12). While the trend of both experimental and theoretical curves is identical, a certain discrepancy (offset) of approximately 5.5 N between them can be observed throughout the whole displacement range. This is mainly caused by friction between the Bowden cables and tendons and flexibility of bands, which introduces a

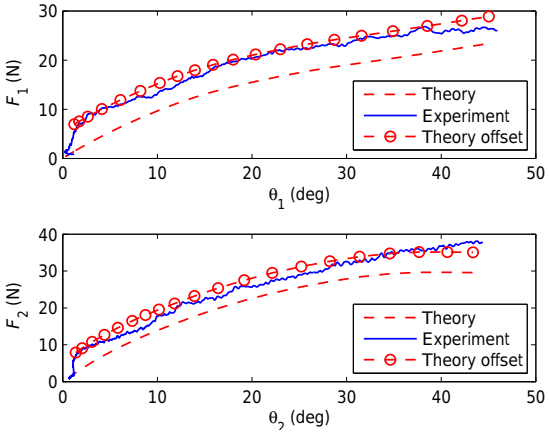

Fig. 9. Comparison between experimental and theoretical values of tension forces for tendons L_1 (top) and L_2 (bottom). Curves labeled 'Theory offset' are plotted taking into account the effects of friction and flexibility of the device.

spring-like effect between tendons and the arm. It can be noted that the offset gradually increases with the increase of angles θ_1 and θ_2, which coincides with spring behavior. This offset can be estimated before operation and introduced into the force model (12), and Fig. 9 also depicts a theoretical curve with such offset estimation. The average RMS error between theoretical and practical values was found to be 2.17 N for F_1 and 2.7 N for F_2, respectively. In addition, the efficiency of the overall transmission mechanism was experimentally found to be in the vicinity of 70 %.

After experimental verification of the proposed force model (12), we used the model for further analysis of shoulder joint forces distribution. Fig. 10 shows the relations between required pulling force F_1 and shoulder angle θ_1 for various positions of point B along y_0 axis and for three different cases of upper arm angles θ_2 (0°, 25° and 55°, correspondingly). The family of characteristics depicted in Fig. 10 may provide important insights on the optimal placement of the pulleys. For instance, it can be observed that, in case of $\theta_2 = 0°$, the motors will require to provide less pulling force for greater values of pulley position y_B, which may drastically decrease power consumption of the device for this particular value of angle θ_2. It can be also observed from Fig. 10 that, with increase of angle θ_2, the value of pulling force F_1 decreases, since a larger quotient of the required force is now provided by the second tendon, F_2. In addition, the shape of the curves also changes, with different values of pulley offset y_B being optimal for $\theta_2 = 25°$ and $\theta_2 = 55°$.

In order to calculate the pulley placements that are optimal for each individual shoulder angle θ_1 and θ_2, one can integrate the curves depicted in Fig. 10 and find the offsets corresponding to the minimal values of this integrals. Such calculated integral values are depicted in Fig. 11 in

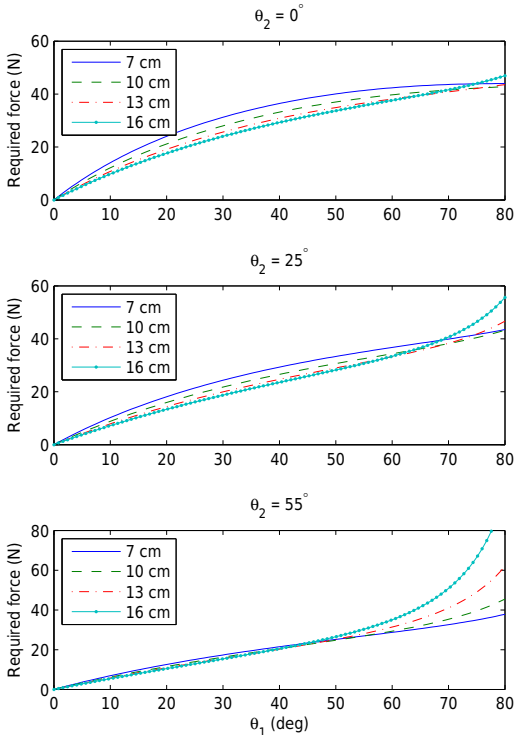

Fig. 10. Families of tendon forces F_1 required to position the elbow in the range of angle $\theta_1 = [0° \;\; 80°]$ for three different cases of angle θ_2.

case of tendon force F_1. The force was integrated with respect to θ_1 over the range of pulley positions y_B between 3 cm and 21 cm. Therefore, Fig. 11 can serve for selecting optimal offset values of point B with respect to angle θ_2. Since the tendons are placed and operate in mutually orthogonal planes, the same logic can be used to select optimal position of the pulley A for tendon L_2.

A few conclusions can be drawn from Figs. 10 and 11. Firstly, the best performance of the exosuit (in terms of minimizing required motor power) can be achieved if offsets of pulleys A and B are made variable and are changed depending on the current position of the shoulder θ_1 and θ_2. We are planning to address this issue in our future work. Secondly, there is a trade-off between the maximum required motor torque and power consumption of the system. For instance, it can be seen in Fig. 10 that, by selecting the value offset to be small, the exosuit will require greater pulling force (and thus more energy) while operating at small values of angle θ_1 and θ_2. At the same time, it might be possible to use a more compact motor, since the maximal pulling force required for large values of angle θ_2 is less.

3.5. Elbow kinematics

Elbow joint with its actuating tendon are schematically presented in Fig. 12. Assuming elbow angle α to be zero when the elbow joint if fully extended, one can find it sim-

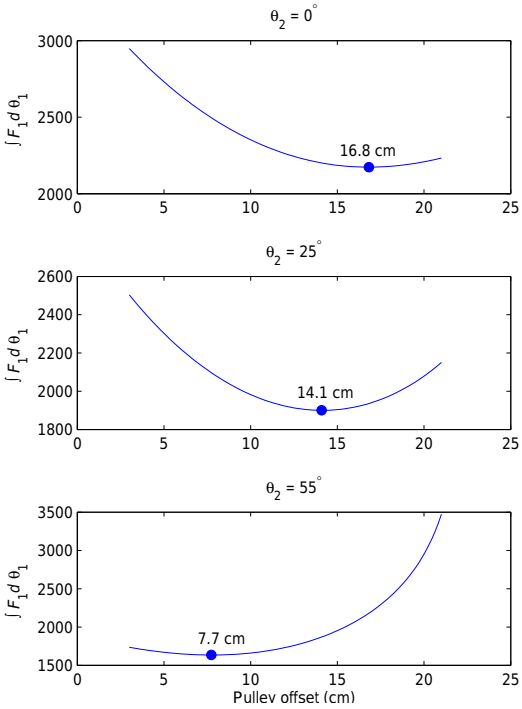

Fig. 11. Comparison of experimental and theoretical values of tension forces for tendons L_1 (top) and L_2 (bottom).

ply as

$$\alpha = 180^\circ - \alpha_1 - \alpha_2 - \alpha_3, \tag{13}$$

where angles α_1 and α_3 are constant values which depend on position of cable insertion points at the arm, namely, upper and lower arm lengths u and l and respective offsets u_{off} and l_{off}. In the practical Auxilio device, the values of angles α_1 and α_3 were calculated to be approximately 13° and 39°, and therefore these angles can not be neglected in the elbow kinematics. Angle α_2 is uniquely determined by the tendon length c and can be found from the resulting triangle via the law of cosines, e.g. $\alpha_2 = \cos^{-1}\left(\left(a^2+b^2-c^2\right)/2ab\right)$, where the quantities a and b are constant and can be calculated with the knowledge of the aforementioned cable connection point coordinates, and tendon length L_3 is assumed to be known.

4. REHABILITATION SIMULATION EXPERIMENT

Based on the results of kinematics evaluation and force analysis obtained for the mechanical arm, we designed a wearable version of Auxilio exosuit and performed a preliminary human study on 4 healthy subjects.

4.1. Wearable exosuit testbed

Figure 13 demonstrates the back view of the prototype of the proposed exosuit when worn on the human. The

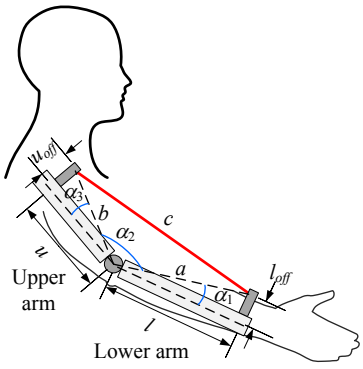

Fig. 12. Schematic representation of the elbow joint used for derivation of elbow kinematics.

system incorporates the main frame worn on the back of the wearer, and two Maxon RE30 motors equipped with 18-to-1 gears and 1024-CPT encoders are installed on the frame. These motors are accountable for twisting inextensible Dyneema strings (8 strings with the effective bundle radius of 1 mm and the length of 23.5 cm) which are connected to the Sava metal cables that represent tendons L_1 and L_2. Bundles of Dyneema strings are connected to the motor shafts at one end and to Sava metal cables on the other. Separators are used in order to prevent twisting of the metal Sava cable [15]. Once Dyneema strings are being twisted or untwisted, this generates linear contraction of tendons L_1 and L_2, which was measured by encoders, as shown in Fig. 13. Sava metal cables travel to the arm band through the Bowden sheaths in order to minimize friction along their path and interference from the human arm motion. The Bowden cables were attached to the frame at points A_p and B_p on the frame side and to the points A and B at the upper arm side. The arm bands were tightly attached around the subject's upper arm by means of a sling-like arm band. No noticeable band slippage was registered during the experiments. However, arm bands still provided some degree of flexibility, which may have negatively affected the accuracy of the system.

4.2. TSA kinematics evaluation

Before moving on to the evaluation of the exosuit kinematics, we experimentally verified the accuracy of the twisted string actuator's model. The following experiment was conducted: motors were commanded to change the lengths of the respective strings according to desired laws generated by the model (1). During the procedure, motor angles and tendon contraction were measured and recorded.

Fig. 14 shows a sample comparison between measured contraction of the tendon and predicted contraction. The predicted and measured values correlate satisfactorily, with the RMSE calculated to be 0.97 cm (11.7 %). Since all TSAs use the string bundles of the same radii

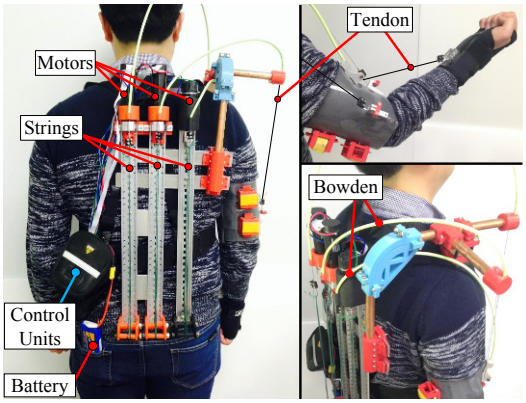

Fig. 13. Auxilio exosuit worn on a human subject.

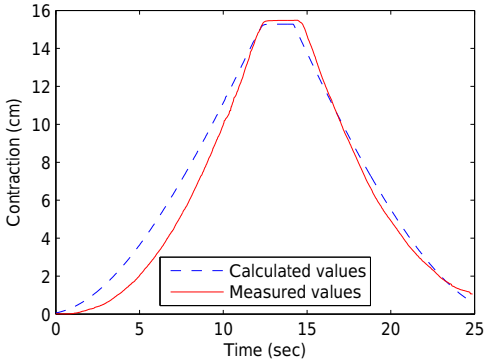

Fig. 14. Kinematics of the twisted string actuator implemented in the proposed exosuit system.

and lengths and incorporate the same motors, all three TSAs performed with identical errors. This error was mainly caused by the inherent hysteresis behavior of the TSAs. Another reason causing the mismatch can be the slack in the strings that occurs during prolonged operation due to the slippage of the harness and the flexibility of the suit. The slack issue can be dealt with by pre-twisting the strings before the operation and taking this pre-twisting angle into account in the TSA model.

Although a certain error in TSA positioning was observed during contraction, we considered low weight, absence of noise and device compliance, all of which originate from the implementation of the TSA in the proposed system, to outweigh possible accuracy issues.

4.3. Elbow kinematics evaluation

We developed a wearable testbed that could actuate the elbow joint and measure its angular displacement.The testbed incorporated a rotary encoder (Autonics E40H12-5000) which measured elbow angle θ_3 and Maxon RE30 gearless motor with encoder (L type, 1024CPT) which was installed on a rigid frame worn on the back (next to the motors for shoulder actuation). Bowden cable was attached to the frame at one side and to the sling-like harness

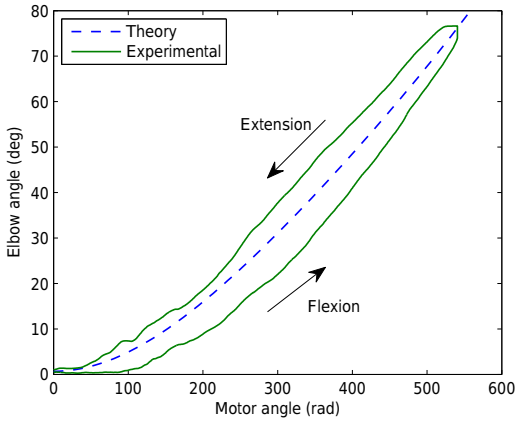

Fig. 15. Kinematics of the proposed exosuit for elbow joint.

worn around the upper arm on the other side. Bundles of Dyneema strings (8 strings with the effective bundle radius of 1 mm and length of 23.5 cm) were connected to the motor shaft at one end and to a metal cable (which represented tendon L_3) on the other. String separator was used in order to prevent twisting of the metal cable. The end of Sava cable was attached to the specially designed glove-like harness which was worn on human hand.

The length of tendon L_3 was determined between two points: upper arm harness, which the Bowden cable was connected to, and the lower arm harness. When the TSA applies pulling force to the tendon, its length L_3 decreases and the elbow angle θ_3 increases. The following procedure was done in order to evaluate (13):

- The motor and twisted string actuator contracted the tendon L_3 until the elbow joint was fully flexed, which in our case corresponded to approximately 78°
- Motor angle and elbow angle were measured and recorded
- Theoretical values of elbow joint angular displacement were calculated using models (1) and (13).

Fig. 15 presents the comparison between practical and calculated values of the elbow angle θ_3. The RMS error between experimental and theoretical data was calculated to be 4.9°. In addition, hysteresis between flexion and extension motion can be observed, which occurred due the inherent properties of TSA and flexibility of the device. However, this error was considered satisfactory for the selected application after the consultation with therapists.

4.4. Simulation of rehabilitation scenario

In this subsection, we present the experimental results of Auxilio's performance in the simulation of the possible rehabilitation scenario.

The original goal of this research project was to develop an assistive device that would be affordable, mechanically simple, light and easy in maintenance, so that more people

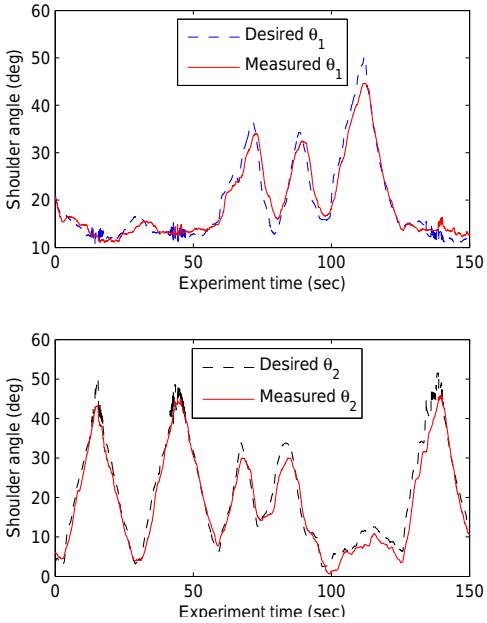

Fig. 16. Time plots of shoulder angles θ_1 and θ_2 during arm following experiments.

who need upper-arm rehabilitation would have the chance to perform (at least partly) their rehabilitation routing at home. One of the most common post-stroke rehabilitation procedures is mirror therapy, which is a simple and inexpensive that was shown to improve upper-extremity function [16, 17]. In addition, this therapy can be performed at home without therapist supervision due to its simplicity and existence of straight-forward visual cues. In the proposed version of the mirror therapy, the patient could exercise his or her affected arm by using the healthy limb as a reference input. The experimental scenario was as follows: A patient wears an exosuit on the affected (slave) arm while facing the motion input sensor device. The control program reads the position of the healthy (master) arm and commands the exosuit bring the injured other arm into the same position, by copying of θ_1 and θ_2 angles using developed kinematics of the exosuit. The angles of humans' upper arm displacement θ_1 and θ_2 were measured via Kinect Xbox 360 motion sensor device, which was placed in front of the human in the experimental scenarios. A Labview Kinect library was used in order to locate the coordinates of humans joints and calculate the angles of arm displacement θ_1 and θ_2. In case if the wearer cannot give a command to the motion sensor with his arm, any assistant with healthy arm can do that for him or her.

The mirroring algorithm works as follows:

- Measured angles θ_1 and θ_2 of the master arm are used as desired values for the exosuit control system.
- The measured values are used to solve the kinematics problem in order to calculate the desired contractions of tendons L_1 and L_2.

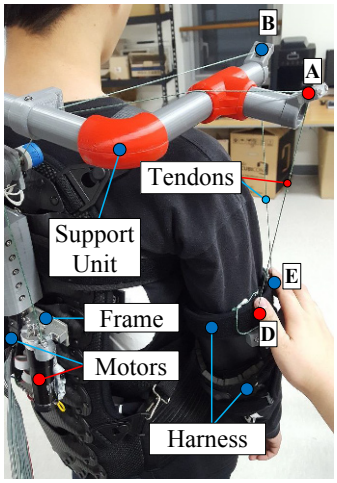

Fig. 17. The latest version of Auxilio.

- The values of tendons contractions L_1 and L_2 are being converted to the desired motor angles λ_1 and λ_2 via the TSA model (1) and sent to motors control systems.
- Finally, the displacement of the slave arm, positioned by the exosuit, is recorded by a motion input device.

The comparison between the angles of displacements of master and slave arms is presented in Fig. 16. It can be seen that the proposed exosuit and kinematics provide an accurate mirroring of the arm's motion. The RMS errors between master and slave arms were 2.12° (9.93 %) for θ_1 and 3.05° (12.47 %) for θ_2.

4.5. Ongoing work

We are currently working on enhancing the capabilities of the proposed device. One direction that we are exploring is designing a single system that can assist people with left-side or right-side paresis, without the need to switch the exosuit for different affected sides. In order to achieve that, we introduced a simple rotational axis and position lock mechanism that allows for easy 'flipping' and locking of the over-shoulder cable support unit from one side of the exosuit to the other, without the need of extra tools. Rigid Bowden cable insertion points A and B are substituted by swivels which prevent cable entanglement and allow free rotation. The top part of the device in different configurations is shown in Fig. 4.

We are also working on improving the ergonomics and portability of the single-sided version of the device, with the latest prototype shown in Fig. 17. Just like the previous version, the developed system assists 3 DOF of upper extremity motion, namely, shoulder joint flexion and abduction and flexion of elbow. The total weight of the system is less than 4 kg: the wearable parts for the upper and lower arms weight 0.32 kg, the mass of the back plate with actuators is 2.8 kg, and the rest of the weight is contributed by control electronics and battery.

Table 3. Specifications of Auxilio.

Range of motion	80° (shoulder abd., flex.) 75° (elbow flexion)
Shoulder flex. time	5 sec
Avg. cable speed	4.9 cm/sec
RMS angle errors	2.12° (shoulder flexion) 3.05° (shoulder abduction) 4.9° (elbow flexion)
Maximum payload	10 kg
Device mass	3.2 kg

5. CONCLUSION AND FUTURE WORK

In this study, we described a fully portable exosuit for shoulder and elbow movement assistance. The exosuit was named Auxilio. The device is light, compact, and easily adjustable and provides assistance for shoulder flexion and abduction, as well as elbow flexion. The total weight of the latest version of the exosuit is under 4 kg, which includes the frame, motors, control unit, and battery. Auxilio was designed for rehabilitation purposes allowing such motions as banding, seating and moving overground. This paper describes a working principle and kinematics of the device and provides insights on the force generated by the exosuit throughout its workspace. Derived kinematic and force relations were confirmed through an extensive experimental study. In addition, the wearable version of Auxilio was tested in the rehabilitation simulation experiment. Despite being soft and flexible, the device demonstrated that it could be positioned with maximal errors of approximately 3° for the shoulder joint and 5° for the elbow joint.

Our future work includes two principal directions. Firstly, we want to integrate a human intention algorithm into the Auxilio device, so that it can be directly controlled by the motion of the wearer's arm, e.g. by analyzing EMG signals from the arm's muscles. As of now, the exosuit can be operated by a pre-defined set of position commands or in a mirroring mode, during which the control system tracks motion of the healthy arm and 'mirrors' its position onto the disabled limb.

Another important direction of our future work is an nsive human study of Auxilio. We are preparing to start human trials on stroke patients in the near future. Finally, our collaboration with therapists shows promises for the proposed system to be used in such exercises as arm stretching, mirror therapy and picking and placement of large objects (like a gym ball) with both arms, all of which can be potentially extended to home-based rehabilitation in the future.

REFERENCES

[1] K. Kiguchi, K. Iwami, M. Yasuda, K. Watanabe, and T. Fukuda, "An exoskeletal robot for human shoulder joint motion assist," *IEEE/ASME Transactions on Mechatronics*, vol. 8, pp. 125-135, March 2003.

[2] J. Sulzer, M. Peshkin, and J. Patton, "Design of a mobile, inexpensive device for upper extremity rehabilitation at home," *Proc. of IEEE 10th International Conference on Rehabilitation Robotics, ICORR 2007*, pp. 933-937, June 2007.

[3] G. Rosati, P. Gallina, S. Masiero, and A. Rossi, "Design of a new 5 d.o.f. wire-based robot for rehabilitation," *Proc. of 9th International Conference on Rehabilitation Robotics, ICORR 2005*, pp. 430-433, June 2005.

[4] C. Carignan, J. Tang, S. Roderick, and M. Naylor, "A configuration-space approach to controlling a rehabilitation arm exoskeleton," *Proc. of IEEE 10th International Conference on Rehabilitation Robotics, ICORR 2007*, pp. 179-187, June 2007.

[5] H. Krebs, N. Hogan, M. Aisen, and B. Volpe, "Robot-aided neurorehabilitation," *IEEE Transactions on Rehabilitation Engineering*, vol. 6, pp. 75-87, Mar 1998.

[6] J. Stein, "e100 neurorobotic system," *Expert Rev Med Devices*, vol. 6, pp. 15-19, 2009. [click].

[7] P. Maciejasz, J. Eschweiler, K. Gerlach-Hahn, A. Jansen-Troy, and S. Leonhardt, "A survey on robotic devices for upper limb rehabilitation," *Journal of NeuroEngineering and Rehabilitation*, vol. 11, no. 1, p. 3, 2014. [click]

[8] C. Mavroidis, J. Nikitczuk, B. Weinberg, G. Danaher, K. Jensen, P. Pelletier, J. Prugnarola, R. Stuart, R. Arango, M. Leahey, R. Pavone, A. Provo, and D. Yasevac, "Smart portable rehabilitation devices," *J Neuroeng Rehabil*, vol. 2, p. 18, 2005. [click].

[9] M. Ding, J. Ueda, and T. Ogasawara, "Pinpointed muscle force control using a power-assisting device: System configuration and experiment," *Proc. 2nd IEEE RAS and EMBS International Conference on Biomedical Robotics and Biomechatronics (BioRob)*, pp. 181-186, 2008.

[10] H. Kobayashi and H. Nozaki, "Development of muscle suit for supporting manual worker," *Proc. of IEEE/RSJ International Conference on Intelligent Robots and Systems (IROS)*, pp. 1769-1774, 2007.

[11] J. Stein, K. Narendran, J. McBean, K. Krebs, and R. Hughes, "Electromyography-controlled exoskeletal upper-limb-powered orthosis for exercise training after stroke," *Am J Phys Med Rehabil*, vol. 86, no. 4, pp. 255-261, 2007. [click].

[12] R. A. R. C. Gopura and K. Kiguchi, "Mechanical designs of active upper-limb exoskeleton robots: State-of-the-art and design difficulties," *Proc. of IEEE International Conference on Rehabilitation Robotics, ICORR 2009*, pp. 178-187, June 2009.

[13] G. Palli, C. Natale, C. May, C. Melchiorri, and T. Wurtz, "Modeling and control of the twisted string actuation system," *IEEE/ASME Transactions on Mechatronics*, vol. 18, no. 2, pp. 664-673, 2013.

[14] I. Gaponov, D. Popov, and J.-H. Ryu, "Twisted string actuation systems: A study of the mathematical model and a comparison of twisted strings," *Proc. of IEEE/ASME Transactions on Mechatronics*, vol. 19, pp. 1331-1342, Aug 2014.

[15] D. Popov, I. Gaponov, and J. Ryu, "A preliminary study on a twisted strings-based elbow exoskeleton," in *World Haptics Conference (WHC), 2013*, pp. 479-484, April 2013.

[16] G. Yavuzer, R. Selles, N. Sezer, S. Sütbeyaz, J. B. Bussmann, F. Köseoğlu, M. B. Atay, and H. J. Stam, "Mirror therapy improves hand function in subacute stroke: a randomized controlled trial," *Archives of physical medicine and rehabilitation*, vol. 89, no. 3, pp. 393-398, 2008. [click]

[17] H. Thieme, J. Mehrholz, M. Pohl, J. Behrens, and C. Dohle, "Mirror therapy for improving motor function after stroke," *Stroke*, vol. 44, no. 1, pp. e1-e2, 2013. [click]

Igor Gaponov received his BS degree in Automation and Control from the Kursk State Technical University, Russia in 2006, and his MS and PhD degrees in Mechanical Engineering from Korea University of Technology and Education in 2008 and 2011, respectively. He is currently an Assistant Professor at the Department of Mechanical Engineering, Korea University of Technology and Education. His research interests include exosuits and assistive devices, human-machine interaction, and nonlinear control.

Dmitry Popov received his BS and MS degrees in Robotics and Mechatronics from the Moscow State Technical University "STANKIN" in 2009 and 2011, respectively, and his MS and PhD degrees in Mechanical Engineering from Korea University of Technology and Education in 2011 and 2014, respectively. He is currently a Postdoctoral Research Fellow at John A. Paulson School of Engineering and Applied Sciences, Harvard University. His research interests include robotics, human-machine interaction, and novel actuation systems.

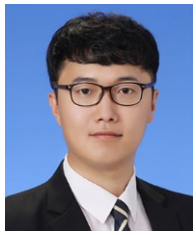

Seung Jun Lee received his BS and MS degrees from the School of Mechanical Engineering at Korea University of Technology and Education, in 2014 and 2016, respectively. His research interests include robotics, automation, control and novel actuation systems.

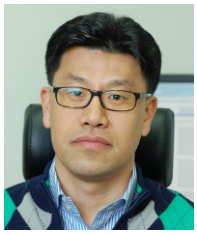

Jee-Hwan Ryu received his BS degree in Mechanical Engineering from Inha University, Rep. of South Korea in 1995, and his MS and PhD degrees in Mechanical Engineering from Korea Advanced Institute of Science and Technology (KAIST), Taejon, Korea, in 1995 and 2002, respectively. He is currently a Professor at the Department of Mechanical Engineering, Korea University of Technology and Education. His research interests include haptics, telerobotics and teleoperation, exosuits, and flexible manipulators.